Toehold-controlled ligation and transcription for accurate COVID-19 genotyping

Yanmin Gao [a,b,c,1], Taoxue Wang [a,b,c,1], Jiaojiao Li [a,b,c], Yanan Wei [a,b,c], Hao Qi [a,b,c,*]

[a] School of Chemical Engineering and Technology, Tianjin University, Tianjin, 300350, China
[b] Key Laboratory of Systems Bioengineering (Ministry of Education), Tianjin University, Tianjin, 300350, China
[c] Zhejiang Shaoxing Research Institute of Tianjin University, Zhejiang, 312369, China

ARTICLE INFO

ABSTRACT

The global pandemic of coronavirus disease 2019 (COVID-19) has significant impact on the entire human society. However, in the face of continually emerging more contagious SARS-CoV-2 variant, the risk to bog down into more severe crisis is around us anytime. Here, we introduce an isothermal, ultrasensitive method for identifying important SNV mutations of SARS-CoV-2. It is based on combined specificity of toehold-assisted linear probe ligation and in vitro transcription signal enlargement, TLT. A ready-to-use panel of TLT assay is developed including detection of 80 crucial SARS-CoV-2 SNVs, by which people could response to the next coming contagious virus variant more rapidly. These advanced point-of-care features make TLT one good approach for large scale population testing of special SARS-CoV-2 variants of interesting.

1. Introduction

Coronavirus disease 2019 (COVID-19) caused by a novel severe acute respiratory syndrome coronavirus 2 (SARS-CoV-2) has posed a serious threat to public health and caused unimaginable social-economic damage worldwide, more than 381 million confirmed cases including nearly 5.6 million deaths around the world as of February 3, 2022 [1]. The low fidelity of RNA polymerase results a high mutation rate in SARS-CoV-2, being estimated about $\sim 1 \times 10^{-3}$ nucleotides per year [2]. SARS-CoV-2 variants are identified with increased transmissibility, high fatality, declined antibody neutralization [3]. For instance, the mutation D614G in spike protein have been proven to be significantly more infectious, and L452R becoming more resistant to neutralizing antibodies [4]. SRAS-CoV-2 variant is specifically classed by a set of SNV mutations [5], and some serious variants are outbreaking around the world [6]. Therefore, there is a need for practical and sensitive detection of single nucleotide variation (SNV). Particularly for large-scale population testing, it is necessary to gain the information about not only if it is SRAS-CoV-2 virus but also what the special variant it is.

Reverse transcription-quantitative polymerase chain reaction (RT-qPCR) is the gold standard in the field of nucleic acid analysis and the major method in current large-scale population SRAS-CoV-2 testing. However, the accuracy of PCR reaction, particularly for genotyping by SNV detection, heavily dependents on expensive thermal cycle machine [7]. Sequencing, thus far, is the major way for accurate genotyping of SRAS-CoV-2. However, as is known to all, it is costly and time-consuming, not appropriate for time-sensitive virus screening of large-scale population. Thus, point-of-care testing with high resolution in SNV detection has great potential in SRAS-CoV-2 testing with capable monitoring on contagious variant.

Here, we developed one isothermal method for genotyping SARS-CoV-2 variant by combining transcription mediated signal reporting and one our previously reported accurate toehold-assisted padlock ligation reaction, toehold-controlled ligation and transcription (TLT). Entropy-driven toehold-blocker is designed to control the assembly of two separate probes on specific target sequence in ligation reaction, in which detection probes only assembles on target sequence with single nucleotide variation while the wild-type sequence is blocked. Following ligation, conjugated detection probes are reported by a transcription reaction. TLT is able to distinguish SNV with a limit of ~ 10 pM on either RNA or DNA target sequence. Furthermore, 80 featured mutations associated with most of major SARS-CoV-2 variants are accurately verified.

2. Methods

2.1. Materials

All the oligonucleotide probes, blocker, and target sequences we used were synthesized at GENEWIZ Inc. (Suzhou, China) and these sequences were listed in Supplementary Tables S1 and S2. Splint R ligase and T4 DNA ligase were obtained from New England Biolabs (Ipswich, MA, USA). Murine RNase Inhibitor was acquired from Vazyme Biotech (Nanjing, China). Malachite green oxalate was purchased from Sigma–Aldrich (Darmstadt, Germany). T7 RNA polymerase was purchased from TaKaRa Biomedical Technology Co., Ltd (Beijing, China). NTPs was obtained from Sangon Biotech. (Shanghai, China). Tris-HCL (pH 7.5) was acquired from Thermo Fisher Scientific (Waltham, Massachusetts, USA). And magnesium chloride solution was obtained from J&K Scientific Ltd. (Beijing, China). ATP was purchased from MDBio, Inc (Taiwan, China).

2.2. Toehold-mediated linear probes ligation

The ligation reaction was carried out in 15 μL reaction mixtures containing 1 × SENSR reaction buffer, Splint R ligase or T4 DNA ligase, linear probe I, linear probe II, the blocker and the target RNA or DNA (specified concentration). Before adding Splint R ligase or T4 DNA ligase, the reaction mixture was denatured at 95 °C for 3 min and cooled to 25 °C at a ramp of 0.1 °C/s using an Eppendorf Mastercycler. After annealing, Splint R ligase or T4 DNA ligase was added and then incubated at 37 °C for 2–3 h.

2.3. Transcription reaction to generate RNA aptamer

The transcription reaction was performed in 30 μL reaction mixtures containing 1 × SENSR reaction buffer, 16 μM Malachite Green, 0.2 U Murine RNase Inhibitor, 2.5 mM NTPs and 100 U T7 RNA Polymerase and 15 μL of the ligation product. The reaction was incubated at 37 °C and fluorescence was measured every 1 min using a Quant Studio 6 Flex Real-Time PCR Systems (Thermo Fisher Scientific, USA).

2.4. SARS-CoV-2 80 well-known mutations detection

For each SNV, linear probes were ligated on DNA target X or target S in the absence or presence of blocker. The ligation reaction was carried out in 15 μL reaction mixtures consisting of 1 × SENSR buffer, 50 U T4 DNA ligase, 100 nM linear probe I, 100 nM linear probe II, 10 nM target X/S, and 0 or 100 nM blocker (without or with blocker in the ligation reaction). The condition of ligation reaction was the same as the toehold-mediated linear probes ligation. After ligation reaction, 15 μL of the ligation product was totally added into transcription reaction system. And the reaction components and condition of transcription was identical to 2.3.

3. Results and discussion

3.1. Toehold-controlled ligation reaction

Recently, we demonstrated one toehold-assisted Padlock ligation [8], in which toehold blocker is designed to control the ligation of one probe sequence to construct circular product. Unlike padlock reaction, in general ligation reaction, two separate probes need to assemble on the target template and thus the thermodynamic process of toehold associated displacement of two separate strands is different [9]. We designed a toehold-controlled ligation reaction for single nucleotide variation (SNV) detection, comprising of two linear probes (I and II) and a toehold blocker. Both of the linear probes are perfectly complementary to wild type DNA (target X) and mutated DNA (target S) and the blocker is perfectly complementary with target X but has a mismatch with target S.

The ligation procedure of target X (upper) and target S (lower) with a single nucleotide variation (blue dot) under toehold control are detailed in Fig. 1A. The two linear probes (I and II) are needed to displace a blocker, which subsequently result in the end-to-end alignment of the two probe strands on the target. Theoretically, the two linear probes ligated on target X or S at almost the same efficiency without the blocker. In the presence of blocker, the branch migration of blocker on target X initiated by toehold of probe I move continuously in one direction and assemble the ligation complex with releasing the blocker, but in the same efficiency the blocker is able to displace the probe to block the assemble of ligation complex (Fig. 1A top). In the case of target S, the mismatch between the target S and the blocker favors the blocker displacement by linear probe I and II and then ligation complex assembly is improved (Fig. 1A bottom). The amount of the ligated products directly reflected the presence or absence of blocker.

To obtain the best discrimination on SNV, a group of blockers (20 blockers in total) were designed with various lengths of the blocker toehold and probe toehold. The blocker was denoted as B (the number of nucleotides of the probe toehold, the number of nucleotides of the blocker toehold) (Fig. 1B). Sequence with one single nucleotide variation of T > G is designed to test the feasibility of toehold-controlled ligation reaction. One linear probe I is labeled with FAM fluorophore at 5′ terminal end and linear probe II is modified with a phosphate group at its 5' terminal end, thus the ligation product can be verified conveniently in the denaturing polyacrylamide gel electrophoresis (PAGE) (Fig. 1C). Linear probes (P) were ligated on target sequence (T) of target X or target S in the presence of various blockers (B) in a molar ratio of P: B: T = 100:100:10, and the ligation products were analyzed and quantified using PAGE (Fig. 1D and Fig. S1). The ligation yield of linear probes on target X or target S were almost the same in the absence of blocker. In contrast, the blocker significantly changed how the probes recognized target X and target S. For all of the blockers, the ligation yield on target S were higher than on target X, and most of blockers significantly favored ligation on target S over target X (Fig. 1D). Because the blocker was designed to perfectly bind with target X, the blocker is able to protect target X much efficient than target S. For the blocker B (5, 5), the highest value 67.5 of the factor Q, describing the capability of variation discrimination (See methods) [8], was obtained. Meanwhile, we note that an efficient template recycling effect in B (5,5) controlled ligation on target S. Theoretically, toehold blocker can make a target strand recycling by removing the ligated product from the target strand. Although ligated products could still react with blocker and the target complex, at least non-ligated linear probes would have almost equal chance to compete.

To explore the potential thermodynamic principle for SNV detection, we analyzed the correlation between the toehold strength of probe toehold and toehold of blocker. The length of blocker toehold was changed while maintaining the toehold of linear probe (sequence in blue) or changing the length of linear probe toehold while keeping the blocker toehold (sequence in red) (Fig. 2A). By plotting the Q value against ΔΔG, it was observed that the Q value gradually increased followed by decreased with the decrease of ΔΔG, namely reducing the length of blocker toehold (blue dots) (Fig. 2B). Meanwhile, the Q value also gradually increased with decreasing ΔΔG when the toehold of blockers kept constant but increased the toehold length of the two linear probes. Although the assay of further decrease of ΔΔG was not identified, due to $\Delta G_{(T\text{-}p)}$ less than $\Delta G_{(T\text{-}b)}$ resulting in quick dissociation of a short blocker from the template, we supposed that the Q value would be decreased. The possible thermodynamic principle will help us to design the blocker and probe for other targets.

3.2. Genotyping SARS-CoV-2 mutation by toehold-controlled ligation and transcription

Based on the toehold-controlled ligation, we designed an isothermal cascade reaction that comprised two successive reactions of ligation and
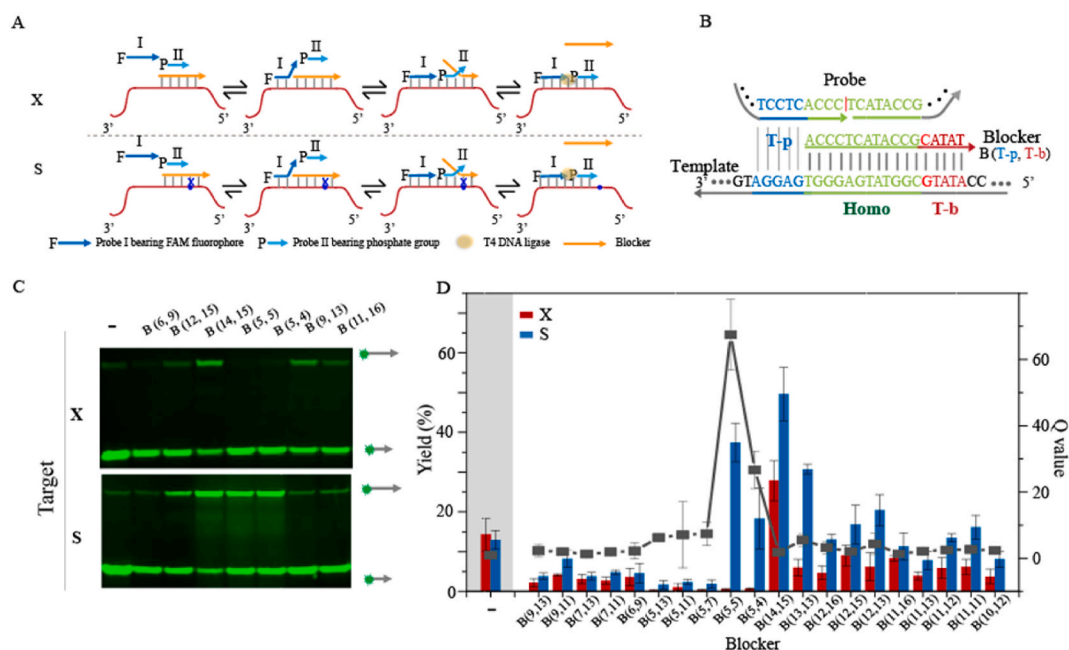
Fig. 1. Toehold-controlled ligation reaction. (A) Illustration of the strand displacement in the linear-probe ligation in the presence of toehold blocker (Blocker strand is marked in orange and probe I/II in blue). **(B)** Schematic of the assembled ligation complex with toehold blocker. The toehold of the linear probes is marked in light blue, the overlapped sequence in green, and the toehold of blocker in red. SNV is in the toehold of blocker (blue dots) and the blocker is denoted as B (T-p, the number of nucleotides in the probe toehold; T-b, the number of nucleotides in the blocker toehold). **(C)** Linear probes were ligated on target X and S by T4 DNA ligase in the presence or absence of various blocker and analyzed in denaturing PAGE. **(D)** The discrimination factor Q (gray square) is calculated from the ligation yield of the linear probes on target X (red column) or S (blue column) in the presence of various blockers. Error bars represent the means ± SD, n = 3. (For interpretation of the references to colour in this figure legend, the reader is referred to the Web version of this article.)
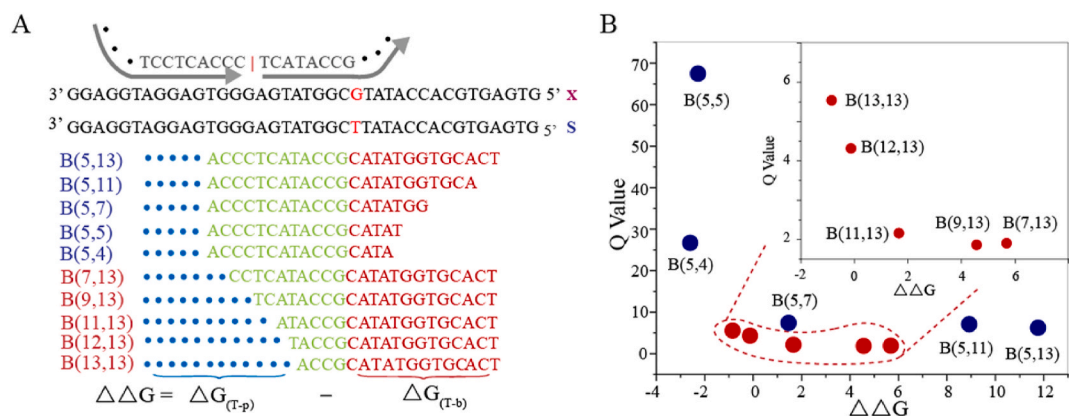

Fig. 2. Thermodynamic of toehold-controlled ligation reaction. (A) The difference of Gibbs free energy ($\Delta\Delta G$) between $\Delta G_{(T-p)}$ and $\Delta G_{(T-b)}$ of 20 toehold blockers were designed. The Gibbs free energy of the probe toehold ($\Delta G_{(T-p)}$) and blocker toehold ($\Delta G_{(T-b)}$) was calculated using NUPACK. **(B)** The discrimination factor Q with various blockers were plotted against the $\Delta\Delta G$ of corresponding toehold blockers.

transcription (Fig. 3A). In TLT, the linear DNA probe I codes one 5′ terminal phosphorylated sequence which is complementary to part of the target sequence and one 3′ terminal stem-loop structured T7 promoter. As previously reported, the stem-loop structure could form an uncommon, active and double-stranded T7 promoter. And as a reporter probe [10], the linear DNA probe II codes a 5′ terminal sequence that is also complementary to part of the target sequence and one 3' terminal sequence that codes sequence for one special RNA aptamer. The two linear probes and blocker competitively bind to the target viral sequence. Being driven by the entropy difference, the linear probe I and II are prone to display the blocker from the mutated target sequence over wildtype sequence forming nucleotide complex for ligation. Once both the linear probe I and linear probe II hybridize perfectly to the target sequence, the two probes are ligated by Splint R ligase. Therefore, the

RNA aptamer on probe II can be directly transcribed from T7 promoter on probe I. And then the produced RNA aptamer can be turned on to fluoresce after specially binding with the malachite green (MG). The fluorescence intensity growth is positively correlated with the amount of ligation products. Therefore, the slope (*k*) of fluorescence signal increasement over the reaction time can be quantified to measure target sequence in sample. If the slope is the same in the presence or absence of blocker, it means there is the special mutation of interest. If the slope become small in the presence of the blocker, it means that the target sequence is the wild type virus sequence and the more target sequence is in the sample the smaller the slope will become. In addition, the influence of T7 promoter and aptamer sequence on ligation were quantified and no significant influence were observed (Fig. S2).

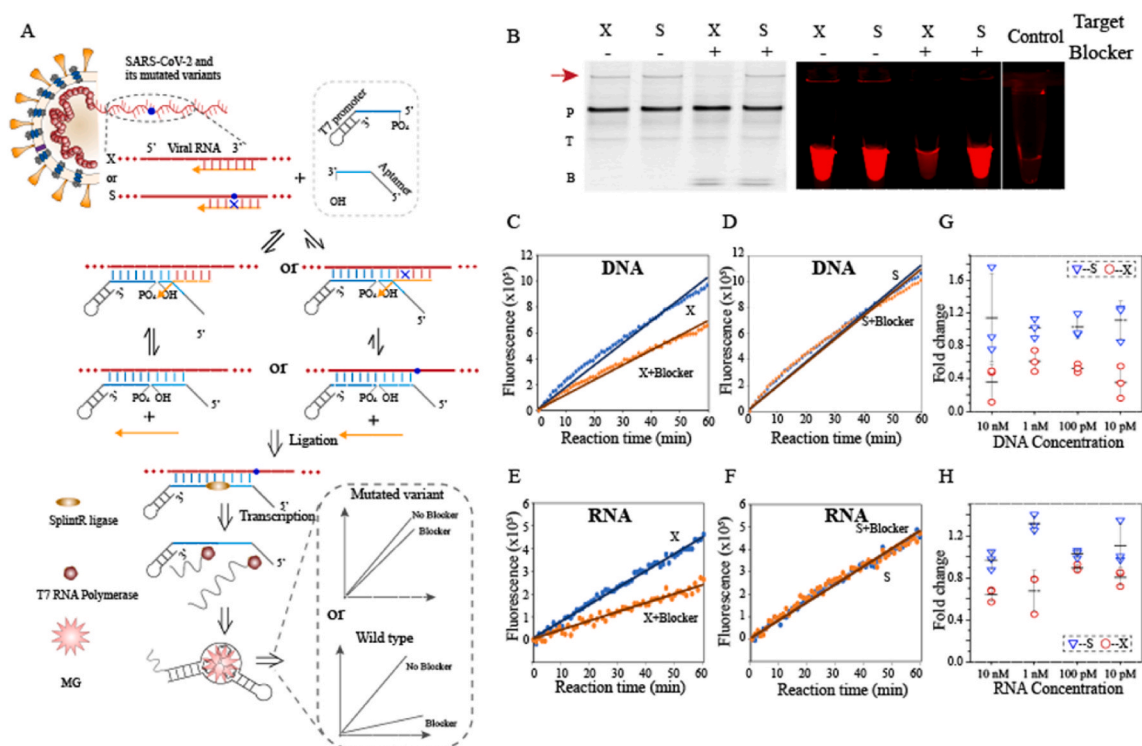The synthesized wild type or variant RNA in the absence or presence

Fig. 3. Toehold-controlled ligation and transcription assay for isothermal genotyping of SARS-CoV-2 variant. (A) Illustration for the general workflow of toehold-controlled ligation and transcription (TLT) assay. (B) Linear probes ligated on synthetic RNA template in the absence or presence of blocker were analyzed in a denaturing PAGE (left). Fluorescence signal were observed after the MG bound to transcription product synthesized by T7 RNA polymerase using the ligated probes as template (right). The fluorescence growth curve of the two linear probes ligated on synthetic DNA target X (C) and S (D) and RNA target X (E) and S (F) in the presence or absence of blocker. Fold change of TLT assay for target DNA (G) or RNA (H) at varying concentrations from 10 pM to 10 nM. All of the tests were performed with three biological replicates.

of blocker were tested and slope k value was measured. We also quantify the fold change from the measured slope value, mathematically expressed as: Fold change $_{(X)} = k2/k1$ and Fold change $_{(S)} = k4/k3$, where $k1$ for wild type target with no blocker; $k2$ for wild type with blocker; $k3$ for variant target with no blocker and $k4$ for variant target with blocker. For a specific SNV and a blocker, Fold change $_{(S)}$ is always larger than Fold change $_{(X)}$. Theoretically, the Fold change $_{(S)}$ should be close to 1 and the Fold change $_{(X)}$ to 0, it indicates that the blocker can identify the SNV while protect the target X. Fold changes $_{(S)}$ with larger than 1 may suggest that the special blocker is good at improving the target recycling in the ligation reaction.

For SARS-CoV-2 L18F mutation (21614 C > T) on the spike protein [11], two linear probes and a blocker of B (13, 8) were designed and synthesized (Fig. S3) and target DNA or RNA were separately synthesized. Two linear probes were ligated on target X or S in the absence or presence of blocker at a molar ratio of I: II: B: T = 100:100:100:10 nM, and the ligated products were analyzed on the denaturing PAGE (Fig. 3B). The amount of ligation products on target X and target S were nearly identical in the absence of blocker; the ligated products on target X were barely visible and the yield of ligated products on target S was more than that on target X in the presence of blocker in the ligation reaction. This result demonstrated that the blocker was prone to bind on target X over target S. Furthermore, after T7 RNA polymerase transcription of ligation product, visible fluorescence signal proved this result again (Fig. 3B). The real-time fluorescence curves of transcription were measured and found that the slope of the fluorescence curve of the two linear probes ligated on DNA target X in the presence of blocker was less than that without the blocker as expected (Fig. 3C). However, for the mutated DNA target S, both fluorescence curves were almost overlapped no matter if the blocker is added or not (Fig. 3D). In addition, target RNAs were also tested using the same linear probes and blocker in the

same ligation and transcription condition, and the very similar results were obtained (Fig. 3E and F). It indicates that TLT is able to work properly on either DNA or RNA target. To further assess the sensitivity of TLT, synthetic DNA and RNA target in the range of 10 pM to 10 nM were tested (Fig. 3 G and H), TLT could consistently detect down to 10 pM of SARS-CoV-2 L18F mutation.

SARS-CoV-2 contains a ~30 kb single-stranded positive-sense RNA as genome, which codes multiple nonstructural proteins, such as viral papain-like proteinase, main protease, RNA polymerase and endoribonuclease, and structural proteins including spike protein, envelope protein, membrane protein, and nucleocapsid protein (Fig. 4A) [12]. Until now, SARS-CoV-2 has been evolving into twelve major classes of variants around the world [13], all of which are characterized by a set of the specific mutations (Fig. 4B). For example, Delta variants (B. 617.2) possesses a unique set of mutations including L452R, T478K and P681R [14]. It has been reported that, since the beginning of SARS-CoV-2 outbreak in late 2019, genome sequencing has showed a nucleotide mutation rate of $\sim 1 \times 10^{-3}$ substitutions per year [2,15]. To a certain extent, these mutations generate variants with high adaptability to environment while easily evading human immune system, the extent of reduction in neutralization by antibodies of previous infection or vaccination. To control the pandemic of SARS-CoV-2, there are critical needs for large-scale testing and genotyping, which allows health services to quickly identify the positive cases, monitor the special variant of interesting.

Based on the SNV discrimination capacity of TLT, we further elaborately designed the linear probes and blockers for a panel of SARS-CoV-2 mutations including 80 the most frequently identified SNVs, all of which were reported to increase viral infectivity, fitness, or interindividual transmissibility. Two linear probes were ligated on target X or S in the absence or presence of blocker at a molar ratio of I: II: B: T =
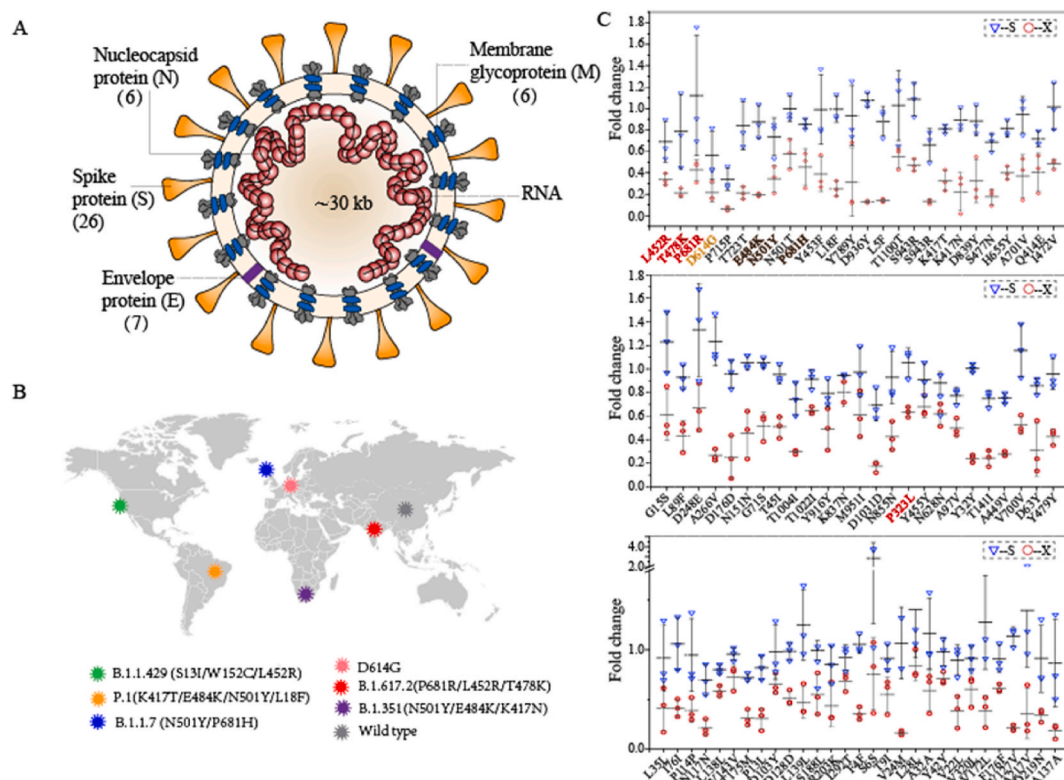
Fig. 4. A ready-for-use panel of TLT assay for SARS-CoV-2 genotyping. (A) The structure of SARS-CoV-2 with crucial mutations in structural and nonstructural proteins. (B) Crucial SARS-CoV-2 variants global map. (C) TLT detection of 80 crucial SARS-CoV-2 SNVs.

100:100:100:10 nM, incubating the reaction mixture at 37 °C for 3h. Then, the T7 RNA polymerase synthesized the RNA aptamer using the ligated products as template at 37 °C for 3h in presence of MG while fluorescence signal was real-time monitored (Fig. S5). Fold changes were calculated and showed in Fig. 4C. It is found that the substitution frequency of T for C is the highest among various types of mutations. These results demonstrated TLT could successfully identify most of important SNVs for identifying the specific SARS-CoV-2 variant. Meanwhile, it was worth noting that the difference between Fold change $_{(X)}$. and Fold change $_{(S)}$. varied significantly for different mutation, indicating that perhaps the secondary structure of target may largely affect the efficiency of TLT. Although we went through a preliminary optimization so that the entire reaction time is only 130 min, containing 120 min for the ligation reaction and 10 min of transcription (Fig. S4), there is still large room for optimization of each reaction steps to save more detection time. These results also provide a valuable insight on designing linear probes and blockers for SARS-CoV-2 SNVs.

4. Conclusion

In the face of emergence of more contagious variant of SARS-CoV-2, there is a critical need for an accurate and efficient genotyping assay in fighting this pandemic. In this study, we present an isothermal, ultra-sensitive method for identifying important SNV mutations of SARS-CoV-2. It is based on the specificity of toehold-assisted linear probes and signal enlargement via in vitro transcription using T7 RNA polymerase. Without target preamplification, the detection limit of this method was down to picomolar level. Although nucleic acid ligation is relative slow reaction, the whole TLT process still rival that of RT-qPCR but with advantage features as point-of-care assay and there is still large room for improvement by such as ligase engineering. A ready-to-use panel of TLT assay is developed including detection of 80 crucial SARS-CoV-2 SNVs, by which people could response to the next coming contagious virus variant more rapidly. However, the difference between Fold change $_{(X)}$.

and Fold change $_{(S)}$. varied largely between different mutations. 71 mutations were quantified with statistical significance $P < 0.05$. But 3 mutations, N628 N, S188L and D103Y, have $P > 0.05$, probably because the influence of secondary structure of target. These advanced features make TLT one good approach for large scale population testing of special SARS-CoV-2 variants of interesting.

CRediT authorship contribution statement

Yanmin Gao and **Taoxue Wang** contributed equally to this work. **Yanmin Gao** and **Taoxue Wang**: Conceptualization, Methodology, Data curation, Writing-original draft. **Jiaojiao Li** and **Yanan Wei**: Investigation, Validation. **Hao Qi**: Project administration, Funding acquisition, Supervision, Writing-review & editing.

Declaration of competing interest

The authors declare no competing financial interests.

Appendix A. Supplementary data

Supplementary data to this article can be found online at https://doi.org/10.1016/j.ab.2022.114803.

References

[1] S. Elbe, G. Buckland-Merrett, Glob. Chall 1 (1) (2017) 33–46.

[2] S. Duchene, L. Featherstone, M. Haritopoulou-Sinanidou, A. Rambaut, P. Lemey, G. Baele, bioRxiv Preprint, 2020.

[3] Genotype to phenotype Japan C. Motozono, M. Toyoda, J. Zahradnik, A. Saito, H. Nasser, T.S. Tan, I. Ngare, I. Kimura, K. Uriu, Y. Kosugi, Y. Yue, R. Shimizu, J. Ito, S. Torii, A. Yonekawa, N. Shimono, Y. Nagasaki, R. Minami, T. Toya, N. Sekiya, T. Fukuhara, Y. Matsuura, G. Schreiber, C. Ikeda, T. Nakagawa, S. Ueno, T, K. Sato, Cell Host Microb. 29 (7) (2021) 1124–1136.

[4] B. Zhou, T.T.N. Thao, D. Hoffmann, A. Taddeo, N. Ebert, F. Labroussaa, A. Pohlmann, J. King, S. Steiner, J.N. Kelly, J. Portmann, N.J. Halwe, L. Ulrich, B. S. Trueb, X. Fan, B. Hoffmann, L. Wang, L. Thomann, X. Lin, H. Stalder, B. Pozzi, S. De Brot, N. Jiang, D. Cui, J. Hossain, M.M. Wilson, M.W. Keller, T.J. Stark, J. R. Barnes, R. Dijkman, J. Jores, C. Benarafa, D.E. Wentworth, V. Thiel, M. Beer, Nature 592 (7852) (2021) 122–127.

[5] R. Wang, Y. Hozumi, C. Yin, G.W. Wei, Genomics 112 (6) (2020) 5204–5213.

[6] M.F. Boni, P. Lemey, X. Jiang, T.T. Lam, B.W. Perry, T.A. Castoe, A. Rambaut, D. L. Robertson, Nat. Microbiol. 5 (11) (2020) 1408–1417.

[7] Y. Wang, H. Kang, X. Liu, Z. Tong, J. Med. Virol. 92 (6) (2020) 538–539.

[8] Y. Gao, H. Qiao, V. Pan, Z. Wang, J. Li, Y. Wei, Y. Ke, H. Qi, Biosens. Bioelectron. 179 (2021), 113079.

[9] A.J. Genot, D.Y. Zhang, J. Bath, A.J. Turberfield, J. Am. Chem. Soc. 133 (7) (2011) 2177–2182.

[10] C.H. Woo, S. Jang, G. Shin, G.Y. Jung, J.W. Lee, Nat. Biomed. Eng. 4 (12) (2020) 1168–1179.

[11] J.D.A. Yasunori Watanabe, Daniel Wrapp, Jason S. Mclellan, Max Crispin, Science 369 (2020) 330–333.

[12] Y. Finkel, O. Mizrahi, A. Nachshon, S. Weingarten-Gabbay, D. Morgenstern, Y. Yahalom-Ronen, H. Tamir, H. Achdout, D. Stein, O. Israeli, A. Beth-Din, S. Melamed, S. Weiss, T. Israely, N. Paran, M. Schwartz, N. Stern-Ginossar, Nature 589 (7840) (2021) 125–130.

[13] W.T. Harvey, A.M. Carabelli, B. Jackson, R.K. Gupta, E.C. Thomson, E.M. Harrison, C. Ludden, R. Reeve, A. Rambaut, C.-G.U. Consortium, S.J. Peacock, D. L. Robertson, Nat. Rev. Microbiol. 19 (7) (2021) 409–424.

[14] A. Saito, T. Irie, R. Suzuki, T. Maemura, H. Nasser, K. Uriu, Y. Kosugi, K. Shirakawa, K. Sadamasu, I. Kimura, J. Ito, J. Wu, K. Iwatsuki-Horimoto, M. Ito, S. Yamayoshi, S. Ozono, E.P. Butlertanaka, Y.L. Tanaka, R. Shimizu, K. Shimizu, K. Yoshimatsu, R. Kawabata, T. Sakaguchi, K. Tokunaga, I. Yoshida, H. Asakura, M. Nagashima, Y. Kazuma, R. Nomura, Y. Horisawa, K. Yoshimura, A. Takaori-Kondo, M. Imai, S. Nakagawa, T. Ikeda, T. Fukuhara, Y. Kawaoka, K. Sato, bioRxiv Preprint, 2021.

[15] T.P. Peacock, R. Penrice-Randal, J.A. Hiscox, W.S. Barclay, J. Gen. Virol. 102 (4) (2021), 001584.